Numerical Study on Effect of Number of Injectors on Scramjet Combustor

Seung-Min Jeong, Jae-Eun Kim, Bu-Kyeong Sung, and Jeong-Yeol Choi
Pusna National University
Busan, 46241, Korea

1 Introduction

High-speed Air breathing propulsion systems, such as Supersonic or hypersonic engines, have made significant advancements over the past decade and are currently in the practical implementation or immediate pre-commercialization phase. However, several issues still need to be addressed, e.g., low-frequency combustion oscillation or instability[1-8] and enhancement of fuel/air mixing. One of these issues, the problem related to fuel/air mixing, arising from the short residence time of the flow in the ram/scramjet combustor, is closely related to the dynamics of the injected fuel. Numerical and experimental studies have been conducted to investigate the dynamics of transverse injection on high-Mach number flow[9-14]. These studies have revealed the local dynamic behavior of the injected fuel, such as small/large scale vortex roll-up and counter-rotating vortex pair et al.

However, in propulsion systems utilizing engines such as ram/scramjets or dual-mode ramjets, multi-injectors are commonly employed instead of a single-injector to enhance combustion efficiency and achieve sufficient thrust needed. Therefore, it is necessary to investigate and compare the dynamics of injected fuel for both single and multiple injectors to determine the influence of injector schemes. In addition to studying the dynamics in the vicinity of the injectors or around the cavity close-out region, it is also important to investigate the combustion dynamics across the entire combustor when changes are made to the fuel injector scheme. However, comprehensive studies that analyze the changes in flame structure and combustion characteristics across the entire combustor depending on various fueling schemes are still rare. In this context, this study aimed to investigate the combustion characteristics and performance associated with changes in the fueling schemes using comprehensive high-resolution numerical analysis.

2 Methodology

The experimental test configuration of Pusan national university's hydrogen-fueled direct-connect scramjet combustor (PNU-DCSC) is depicted in Fig. 1. PNU-DCSC is consist of three parts: small rocket type vitiation air heater (VAH), shape transition nozzle and scramjet combustor. VAH has single shear co-axial gaseous hydrogen/oxygen injector. VAH has twenty-four of hole type air injectors located along

Correspondence to: aerochoi@pusan.ac.kr

Fig 1: Experimental configuration of Pusan National University-direct connect scramjet combustor (PNU-DCSC).

the outermost radial direction of the injector head for composition of vitiated air and gaining the film cooling effect on the chamber wall side. The design point of inflow of the isolator is Mach number of 2.0 and static temperature of 1,000 K. The cross-sectional area of the isolator is 20 mm × 20 mm. Total length of scramjet combustor from the isolator entrance to combustor exit is 750 mm.

The target of present study is effect of fueling scheme on the combustion characteristics and performance, such as combustion efficiency. To figure out the effect of number of injectors, we set the single- and three multi-injectors under the similar range of global equivalence ratio (ER) condition. Single-injector has a single-injector hole with 2.6×2.3 mm^2, instead, the multi-injector has three injector-hole with 1.4×1.3 mm^2. Both fueling schemes have the same injector pressure ranges to keep the similar ER condition to each other. Detailed information of working fluid and fuel injection condition is noted in Table 1.

Present study utilized density-based fully compressible reactive flow in-house solver, called "RPL3DFR". Chemical species, momentum, and energy conservation equations, in which a fluid and chemical reaction are fully coupled, were used as the governing equations. All governing equations with Favre-filtered of the conserved variables were treated via the finite volume method. Present solver is based on a finite-rate approach; therefore, density was calculated by sum of the partial density of each radical. The improved delayed detached eddy simulation (IDDES) model was used as the turbulence model. Jachimowski's detailed hydrogen/air laminar chemical mechanism, which is composed of 8 species and 19 reaction steps, is used as chemistry. Reaction source term is treated using quasi-laminar approach. Owing to fine grid resolution (x-direction≈(Δ~0.009 mm) and y-direction≈(Δ~0.09 mm).) on small volume of the present combustor (O(100 cm3)), grid resolution is smaller than typical size of reaction thickness, therefore, applying the quasi-laminar approach on chemical source term is reasonable in the present simulation.

Table 1: Inflow and fuel injection

		Isolator inlet	Fuel Injection				
		▼	▼				
Mach number		2.0	Sonic condition				
Static temperature		1,200 K	291.15 K				
Static pressure		1.65 bar	3.3 bar	4.8 bar	6.3 bar	7.8 bar	9.3 bar
ER, single-injector		-	≈0.24	≈0.35	≈0.46	≈0.57	≈0.68
ER, multi-injector			≈0.21	≈0.29	≈0.39	≈0.48	≈0.58
Mole fraction	N_2	0.5952	-				
	O_2	0.2227	-				
	H_2O	0.1821	-				
	H_2	-	1.0				

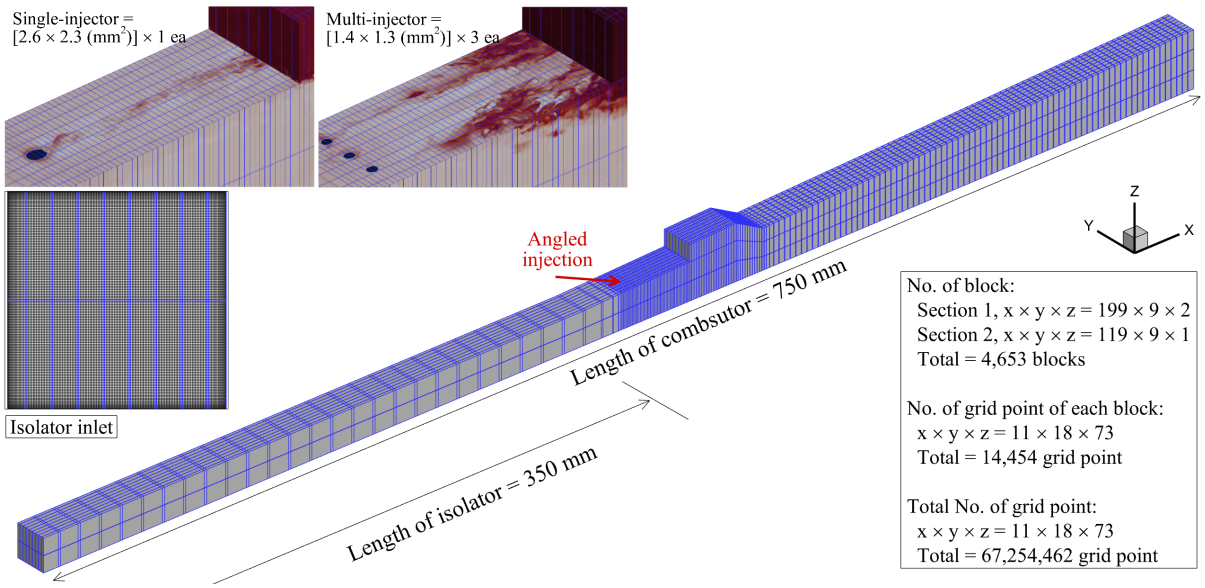

Fig 2: Configuration of the entire computational domain. The block information noted in the figure corresponds with the superfine grid level in the present study.

Convective flux reconstruction was treated by 5th order optimized Multi-dimensional Limiting Process (oMLP) method, and viscous flux are calculated using 4th order centeral differential. AUSMPW+ scheme is utilized on flux splitting method. 2nd order accuracy LU-SGS with maximum 5th steps sub-iteration is applied for time integration.

Coarse (≈7.0 million), medium (≈15.6 million), fine (≈29.6 million), super fine (≈67.2 million) grids were generated for the present simulation. However, we find that only the fine and super fine level can produce high-fidelity results. Therefore, only the results from the super fine grid are used in the present study. The first spacing of the gird at side(Δy) and top-bottom(Δz) wall under the super fine grid is Δy ~7.626×10^{-3} and Δz ~ 8.195×10^{-2} mm, respectively. The computational domain is consisting of the isolator and combustor as depicted in Fig. 2 Domain is divided total of 4,653 blocks for parallel calculation with MPI. We conducted two simulation for validation of present framework; one is for present PNU-DCSC and the another is Evans et al.'s supersonic jet flame. It was confirmed that both numerical results appear good agreement with experimental data.

3 Results and Discussion

In the present study, the qualitative comparison of instantaneous or time-averaged results is using the 9.3 bar of injection pressure result at each injector scheme. Owing to sufficient high enthalpy incoming air, above the static temperature of 1,200 K, auto ignition is made up at entire ER and injector conditions, and this led to the jet-wake stabilized combustion mode as results depicted in Fig. 3. Overall combustion characteristics in Fig. 3 show that well illustrates the typical feature of the jet-wake combustion mode of scramjet combustor.

Interesting point is flame structure, especially flame length along the longitudinal direction of the combustor. The flame length, which can be expressed in contour of heat release rate (HRR), showing the difference in length between the two injector schemes. There is strong HRR distribution along the outermost of the fuel stream in both fueling scheme cases at the fuel injector region. However, after the cavity close-out region at the multi-injector case, HRR is only held on a thin fuel/air mixing layer and the flame length is shortened than the single-injector case. HRR contour and flame length results indicate that the number of injectors or fueling scheme has significant effect on combustion process and its characteristics.

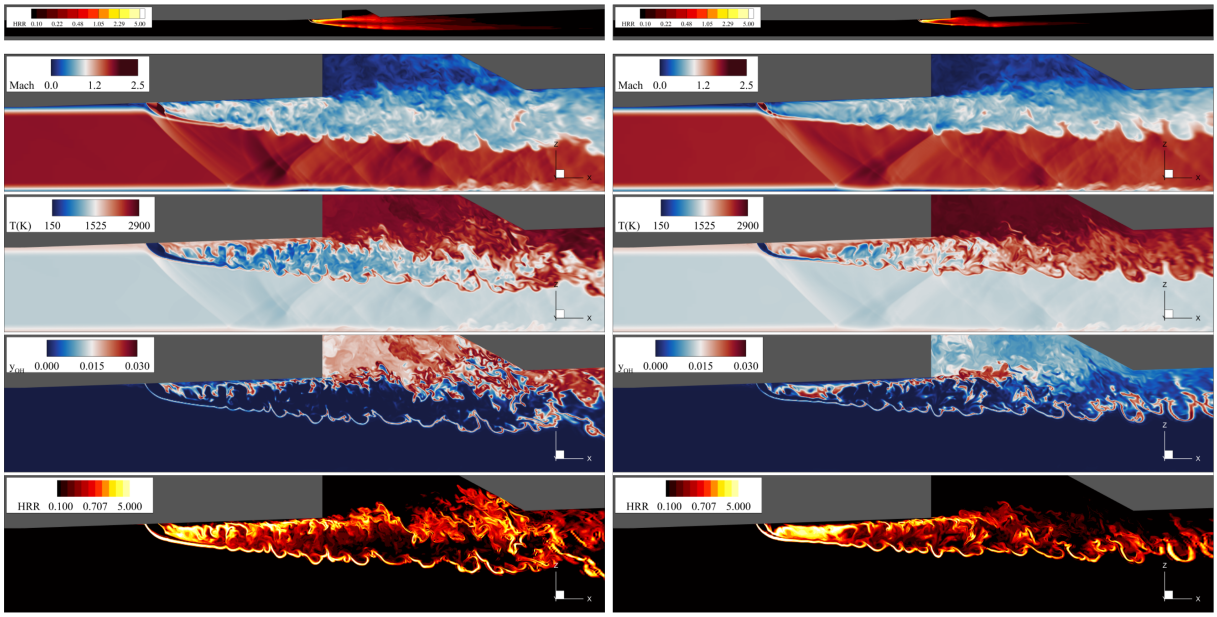

Fig 4: (top) Time-averaged dimensionless heat release rate (HRR) results and (bottom) instantaneous results of Mach number, temperature and HRR; Left side contours are single-injector with injection pressure of 9.3 bar, and right contours are multi-injector with injection pressure of 9.3 bar. Entire contour is from the center-plane (streamwise direction).

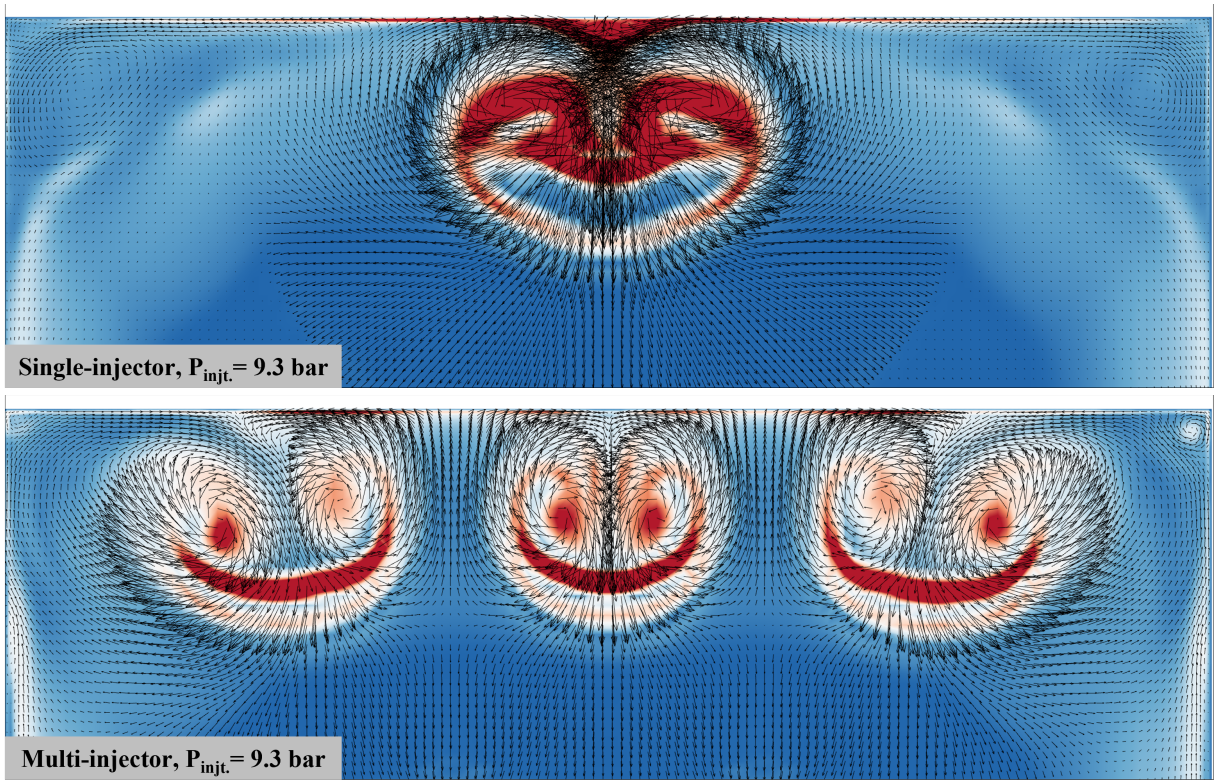

Fig 3: Time-averaged dimensionless vorticity magnitude. Top contour is single-injector case, and bottom contour is multi-injector case, and both cases have same injection pressure with 9.3 bar. The vector line is plotted by streamwise velocity component and high-direction velocity component.

Fig. 4 is non-dimensional vorticity magnitude of YZ plane at near the injector region. Single-injector results show the typical shape of counter-rotating vortex pair (CRVP). However, the multi-injector case show the different dynamics. First, there are interaction between a recirculation flow of the center and side fuel jet's CRVP. The recirculation flow of the side fuel jet of CRVP attempting to return to the upper wall prevents the central fuel jet penetrates the main flow sufficiently, resulting in a loss of momentum of the central jet towards the main flow and insufficient penetration height. Due to interaction with the CRVP structure of the central jet and side wall, the side jet's fuel stream towards the center side of the combustor. Gradually, the side jets entrain towards the center region, leading to a shortening of penetration height and interference between the major recirculation region of the CRVP and the upper wall. The dynamics of the side fuel jets affect the CRVP structure of the central jet, resulting in a loss of momentum in the height direction of the combustor and inducing an insufficient penetration height. The dynamics of the side fuel jets affect the CRVP structure of the central jet, resulting in the central fuel stream loss of momentum in the height direction of the combustor and having an insufficient penetration height. Owing to these characteristics, the CRVP structure of the multi-injector collapses rapidly, and reduction of the fuel/air mixing performance.

Time-averaged OH mass fraction at each YZ plane is depicted in Fig. 5. Before the cavity close-out region ($\leq 39.5\ cm$), both single- and multi-injector case show the CRVP structure, and it can be founded that most reaction process is held on outermost region of the fuel stream. However, at the cavity region($= 43.0\ cm$), the fuel stream of the multi-injector cannot maintain the structure of the CRVP and collapsed. Furthermore, strong OH distribution is detected along the shear layer on the cavity and the region between the side jet and wall surface, whereas the single-injector presents that strong OH mass fraction is anchored inside the cavity. After the cavity close-out region ($\geq 46.5\ cm$), in the case of a single injector, the fuel stream maintains the CRVP structure and tendency to penetrate the primary flow. The OH mass fraction is distributed along the outermost fuel/air contact surface of the penetrated fuel, indicating continuous fuel/air mixing. However, in the case of multi-injectors, owing to the loss of momentum to the combustor height direction, the fuel stream cannot maintain the CRVP structure, and therefore, CRVP completely collapsed. As a result, the fuel stream no longer penetrates the main flow, and fuel/air mixing is decreased. The OH mass fraction is only distributed along the thin flat shape contact surface between the main flow and the fuel stream.

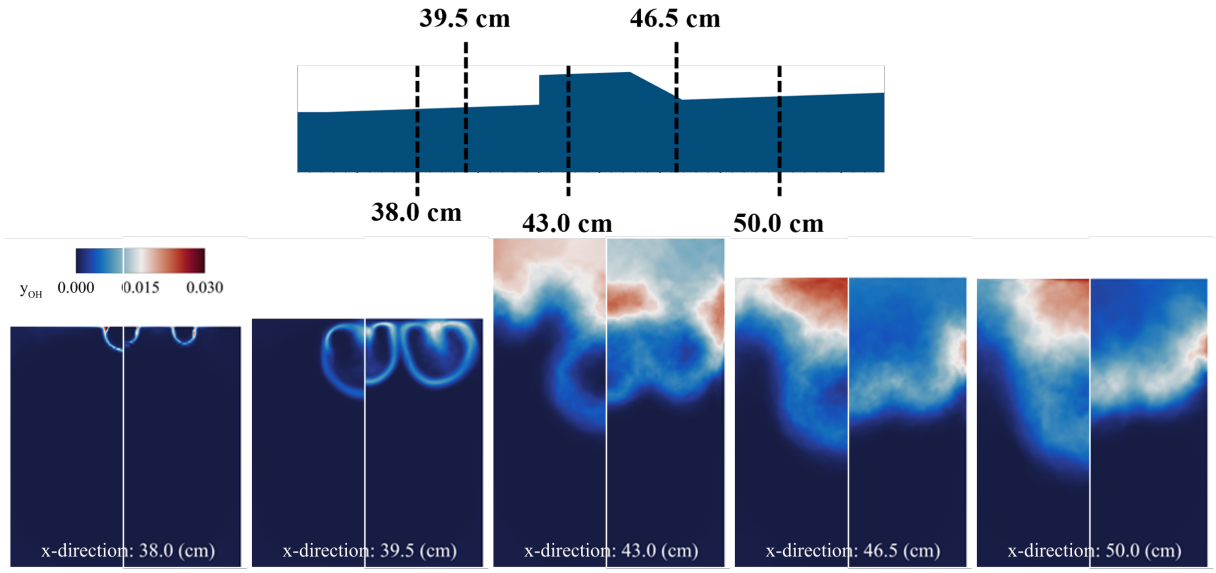

Fig. 5 Time-averaged results of OH mass fraction at each YZ plane. The longitudinal point of each YZ plane is noted at top of figure; left box is single-injector case, and right box is multi-injector case. Both cases have same injection pressure with 9.3 bar.

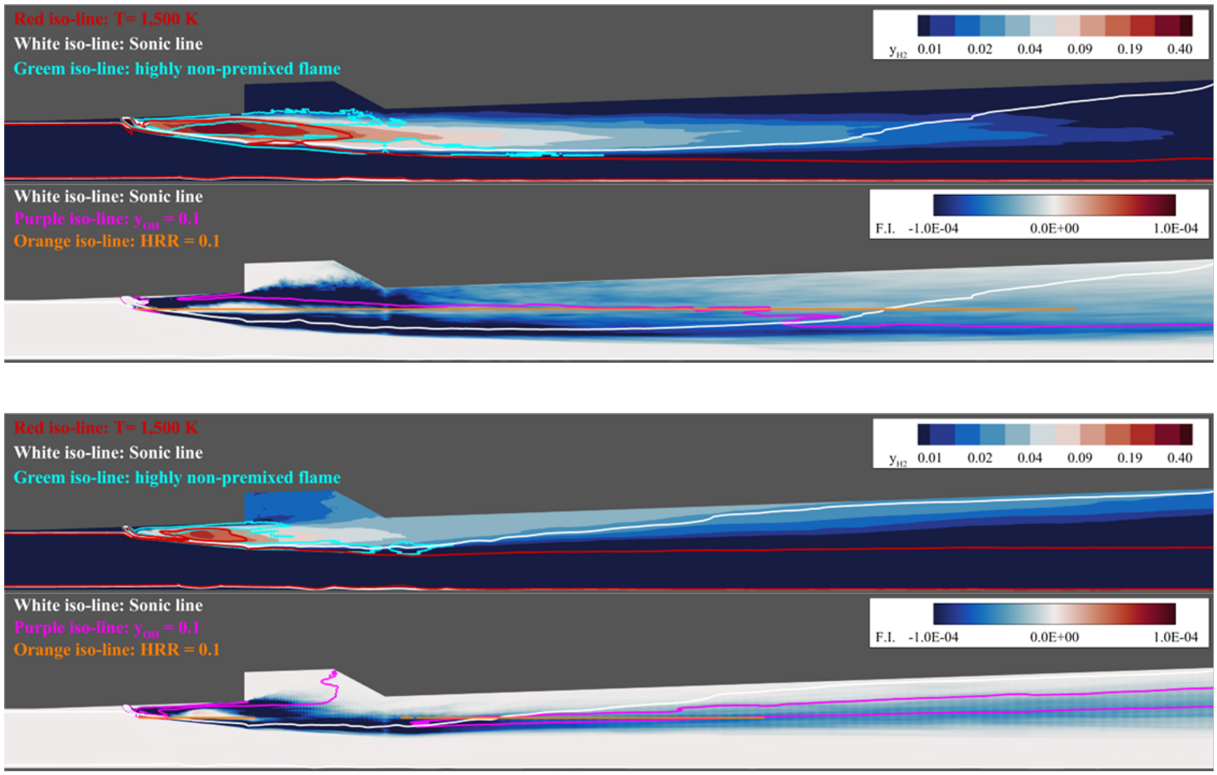

Fig. 6 Time-averaged results of H_2 mass fraction and Takeno flame index. H2 mass fraction is plotted by log-scale. The top two figures are the single-injector case, and the bottom figures are the multi-injector result. Both cases have the same injection pressure of 9.3 bar.

Fig. 6 clearly illustrates the combustion characteristics resulting from the fuel/air mixing performance difference due to the fueling schemes. Firstly, in the case of a single-injector, the fuel stream penetrating the main flow uniformly distributes high-temperature flow fields of 1500 K or higher throughout the height of the combustor. Additionally, most of the injected fuel is consumed at the combustor exit. The flame index indicates a non-premixed flame characteristic along the entire outermost surfaces of the fuel stream, indicating the occurrence of strong fuel/air mixing in those regions. The HRR and OH distribution is also observed homogeneously throughout the entire height of the combustor.

The H_2 mass fraction of the multi-injectors is not fully consumed at the combustor exit. Furthermore, fuel distribution is captured within the cavity, and in the combustor downstream, it exhibits attached distribution on the upper wall. As a result of the relatively low fuel/air mixing performance, the high-temperature flow fields also tend to be skewed towards the upper wall. Although exhibiting non-premixed combustion characteristics, this feature is only observed along the contact surface between the fuel stream and the main flow. The OH mass fraction is captured only within this narrow local region of the combustor.

Fig. 7 shows the combustion efficiency of entire ER cases. When ER is below 0.35, trends of combustion efficiency of the single- and multi-injector shows similarities.

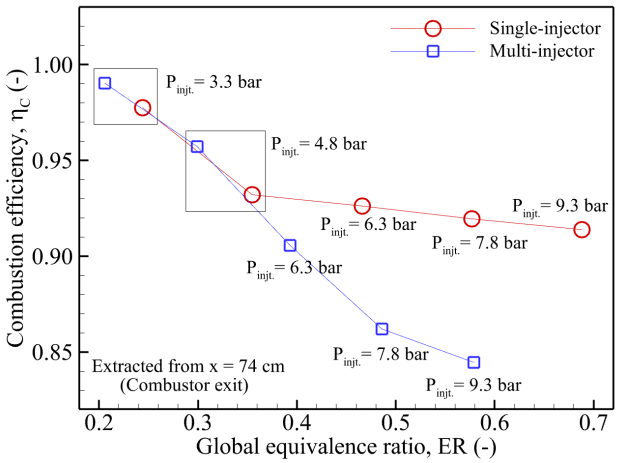

Fig. 7 Combustion efficiency of the entire fueling scheme conditions at the combustor exit

However, when ER is increased more than 0.35, The combustion efficiency of the single-injector is not much reduced and maintained the level. In contrast, the multi-injector case shows that combustion efficiency is reduced considerably. The combustion characteristics of the multi-injector that combustion is only held on the thin fuel/air contact surface induced by the collapse of the CRVP structure and reducing penetration height, leads to a significant reduction in combustion efficiency. Considering that this is a scramjet combustor, the combustion efficiency declined to 0.85 at nominal flight conditions (ER≈0.6), is a fatal issue and, it must be avoided.

4 Conclusion

In this study, high-resolution numerical simulation is conducted to investigate the effect of the number of fuel injectors on the performance of scramjet combustor. Comprehensive numerical results show the possibility exists which is multi-injectors aiming to increase the fuel/air contact surface for improving the mixing-combustion efficiency and enhanced performance, have lower performance compared to a single-injector under similar global ER conditions. The fuel used in the present study is gaseous hydrogen. However, for high hydrocarbon liquid fuels, which are the normal choice of actual propellants for high-speed air-breathing vehicles, the dynamics and combustion characteristics of the injected fuel would be determined by atomization-vaporization-mixing-combustion process or density diffusion resulting from high-pressure injection like supercritical fluid characteristics. Therefore, comprehensive studies (numerical or experimental) are necessary to clearly understand for the combustion dynamics under the multi-injector depending on the fuel characteristic.

References

[1] J.-Y. Choi, F. Ma., V. Yang, Proc. Combust. Inst. 30 (2005) 2851-2858.
[2] K.-C. Lin, et al., J. Prop. Power 26(6) (2010) 1161-1169.
[3] D. J. Micka, et al., AIAA Propulsion and Energy Forum, 2015.
[4] G. Zhao, M. Sun, J. Wu, X. Gu, H. Wang, Aero. Sci. Tech. 87 (2019) 190-206.
[5] J. Lee, N. Yokev, D. Michaels, J. Prop. Power 38(6) (2022) 945-956.
[6] S.-M. Jeong, J. H. Lee, J.-Y. Choi, Proc. Combust. Inst. 39(3) (2023) 3107-3116.
[7] N. Zettervall, K. Nordin-Bates, C. Ibron, C. Fureby, 33rd ICAS, 2022.
[8] S. Guo, X. Zhang, Q. Liu, L. Yue, Physics. Fluids 35 (2023) 45108-45120.
[9] A. Ben-Yaker, M. G. Mungal, R. K. Hanson, Physics. Fluids 18 (2006) 26101-26117.
[10] S.-H. Won, I.-S. Jeong, B. Parent, J.-Y. Choi, AIAA J. 48(6) (2010) 1047-1058.
[11] G.-X. Li, et al., AIAA J. 58(3) (2020) 1216-1226.
[12] K. Wu, P. Zhang, X. Fan, Aero. Sci. Tech. 120 (2022) 107255-107267.
[13] D. Fries, D. Ranjan, S. Menon, J. Fluid Mech. 911 (2021) A45.
[14] A. Mura, A. Techer, G. Lehnasch, Combust. Flame 239 (2022) 111552-111568.